Application of an Advanced Eddy Current Loss Modelling to Magnetic Properties of Electrical Steel Laminations in Wide Range of Measurement

Hamed Hamzehbahmani[1], Philip Anderson[1] and Simon Preece[2]
[1]Wolfson Centre for Magnetics, Cardiff University, Cardiff CF24 3AA, UK
[2]Cogent Power Ltd., Newport NP19 0RB, UK

***Abstract*-- This paper investigates the influence of a wide range of magnetising frequency and peak flux density on the magnetic properties of the electrical steels. In the relevant studies some important factors and operational properties, e.g. skin effect, non-uniform flux density distribution, complex relative permeability and magnetisation characteristic of the material, which are often neglected in the literature, are highlighted. Analytical modelling and experimental works were performed for 3 % grain oriented silicon steel. In order to show the impact of peak flux density on the magnetic properties, two peak flux densities 1.3 T as a high permeability point and 1.7 T as a low permeability point were considered. The results highlighted that magnetising frequency and peak flux density are two determinant factors with significant effect on the magnetic properties of electrical steels.**

Index Terms: Eddy current power loss, equivalent circuit, skin effect, complex relative permeability, high frequencies, loss separation.

1. Introduction

Electrical steels are widely used as the magnetic cores of electrical machines such as transformers, generators and motors. The magnetic cores are constructed from stacks of electrical steel laminations, typically 0.23~0.50 mm thick. In the design and analysis of electric machines, power losses play an important role which is usually divided into three major categories; copper losses, mechanical losses and magnetic losses. The copper loss takes place in the winding of the machine and the mechanical loss arises from the rotation of the machines. The magnetic loss is commonly divided into two components: the eddy current loss and the hysteresis loss and account for a significant portion of the total losses ranging from 15 % to 25 % in machines operating with sinusoidal supplies of 50 Hz or 60 Hz [1-2].

When a magnetic core is exposed to a time-varying magnetic field, an *emf* is induced in the individual laminations of the core, and consequently eddy currents are generated along a closed path inside the laminations. Fig 1 shows the paths for the induced eddy currents in a stack of magnetic laminations exposed to time varying magnetic field. These eddy currents, according to Lenz's law, produce a secondary magnetic field that opposes the applied field. The eddy-current magnetic field is maximum at the centre of the lamination, where the contribution of all eddy currents adds, and minimum at the lamination surface. The actual magnetic field inside the lamination is the summation of the applied field and the eddy-current field. Therefore, distribution of the actual magnetic field is non-uniform across the lamination thickness, being maximum at the surface and minimum at the centre of the lamination. The confinement of the magnetic field around the lamination surface is known as *skin effect* [2]. At low frequencies, the generated eddy currents are small, and skin effect could be neglected. However at high frequencies, skin effect is significant and the peak flux density differs across the lamination thickness. Accurate studies on core losses at high frequencies require skin effect and its consequences on the magnetic properties of the magnetic cores taking into account.

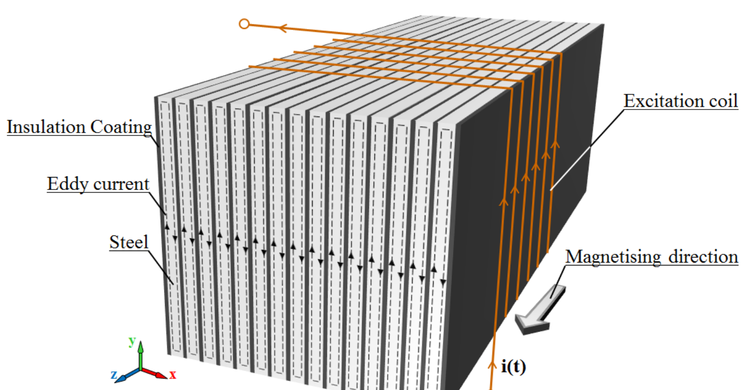

Fig 1 Perspective view of a stack of magnetic lamination under time varying magnetic field

Various analytical and FEM based methods have been developed to estimate core losses [2-14]; non-uniform flux density distribution has been considered in some of these methods [2-6]. Different methods have been also reported based on equivalent circuits of magnetic laminations to predict the magnetic properties of cores [15-17]. Geri et al. [15] proposed an equivalent *RC* electrical network based on the physical dimensions of the laminations to compute the effective permeabilities of multi-laminated thin films in the frequency domain. Loisos et al. [16] implemented an equivalent resistive circuit for magnetic laminations based on the eddy current path in the lamination to study electrical stress on the electrical steel coating. Wang et al. [17] used an equivalent resistive circuit for a stack of laminations to simulate eddy current density in the laminations. Similar concept was implemented in [18-19] to predict magnetic properties of permanent magnet eddy current couplers by modelling the magnetic flux paths with corresponding equivalent circuit.

An analytical model was developed to estimate eddy current power loss of magnetic laminations based on equivalent circuit of eddy current path in the laminations [3]. In this paper, based on this developed model, the influence of a wide range of magnetising frequency and relative permeability on magnetic properties of electrical steels are discussed. In the relevant studies, skin effect, non-uniform flux density distribution, complex relative permeability and magnetisation characteristic of the material (variation of the effective relative permeability with peak flux density) are examined. The analytical modelling and experimental works were carried out using conventional grain oriented (CGO) electrical steel which is widely used in transformer cores.

2. Initial requirements in study of magnetic properties of magnetic materials

A perspective view of a single sheet lamination of thickness $t=2a$ in a magnetic field $B_s \cos \omega t$, applied in rolling direction is shown in Fig 2. In this figure, z and y directions represent rolling and transverse directions, respectively.

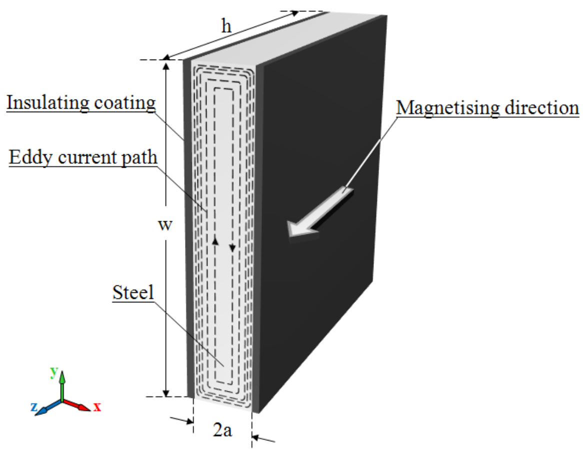

Fig 2 Single strip lamination under time varying magnetic field

If eddy current loops are assumed to be large enough along the y-direction, the field problem becomes one dimensional and can be reduced to a single equation for z-component of magnetic flux density $B_z(x,t)$ that depends on x and t [20]:

$$\frac{\partial^2 B_z(x,t)}{\partial x^2} = \mu_0 \mu_z \sigma \, \frac{\partial B_z(x,t)}{\partial t} \tag{1}$$

where μ_0 is permeability of free space, μ_z is permeability of the material at a particular flux density B_z and σ is electrical conductivity of the material. Equation (1) is a differential equation which defines the flux density B_z as a function of distance x and time t. This equation was solved for a particular relative permeability and magnetic flux density based on the method mentioned in [20]; therefore the instantaneous flux density at any depth inside the lamination is obtained by:

$$B_z(x,t) = B_s \sqrt{\frac{\left(Cosh\,\frac{2x}{\delta} + Cos\,\frac{2x}{\delta}\right)}{\left(Cosh\,\frac{2a}{\delta} + Cos\,\frac{2a}{\delta}\right)}}\; Cos(\omega t - \beta) \tag{2}$$

Equation (2) defines flux density along the thickness of the lamination as a function of distance x, skin depth δ and time t. B_s is flux density at the surface of the lamination, β is phase angle of the flux density and δ is skin depth, which is an important parameter in eddy current modelling and defined by:

$$\delta = \sqrt{\frac{2}{\omega \mu_0 \mu_z \sigma}} = \frac{1}{\sqrt{\pi f \mu_0 \mu_z \sigma}} \tag{3}$$

Equation (3) shows that for a given material with specific conductivity σ, skin effect depends on magnetising frequency f and relative permeability of the material μ_z. Substituting $x=\pm a$ into (2), the flux density at the surface of the lamination is obtained as:

$$B_z(+a,t) = B_z(-a,t) = B_s\; Cos\; \omega t \tag{4}$$

A. Effect of flux density variation on permeability

Equation (2) was obtained from the solution of equation (1) with an assumption of a linear magnetic material. However, the distribution of flux density depends on the magnetic permeability of the material which varies along the hysteresis curve which in turn depends on the peak flux density. The variation of permeability affects the distribution of flux density across the lamination thickness, being non-uniform for high permeabilities and more uniform for low permeabilities at low flux densities and near saturation. To account for the variation of field distribution with the peak flux density, the magnetic permeability is allowed to vary with the peak flux density. Therefore, the permeability is expressed as a fourth-order polynomial [2]:

$$\mu(B) = K_4 B_{pk}^4 + K_3 B_{pk}^3 + K_2 B_{pk}^2 + K_1 B_{pk} + K_0 \qquad (5)$$

where B_{pk} is peak flux density and K_4 to K_0 are curve fitting coefficients obtained from the measured magnetic permeability at low frequency. The relation between the peak value of magnetic field strength H_{pk} and peak value of magnetic flux density B_{pk} is:

$$B_{pk} = \mu_0 \mu_r H_{pk} \qquad (6)$$

The peak magnetising field can be calculated from the measured peak magnetising current I_{pk}, the number of turns of the magnetising coil N_1, and the mean magnetic path length of the magnetic circuit l_m:

$$H_{pk} = \frac{N_1 I_{pk}}{l_m} \qquad (7)$$

Therefore the effective relative permeability μ_r as a function of flux density can then be obtained using the following equation:

$$\mu_r = \frac{B_{pk} l_m}{\mu_0 N_1 I_{pk}} \qquad (8)$$

Based on the equations (7) and (8), the relative permeability of a single sheet lamination of CGO at flux densities 0.1 T to 1.8 T and 50 Hz frequency was measured using a single strip tester (SST); the result is shown in Fig 3. The polynomial function of this curve was obtained by using the polynomial solver of MATLAB, which is shown on the figure.

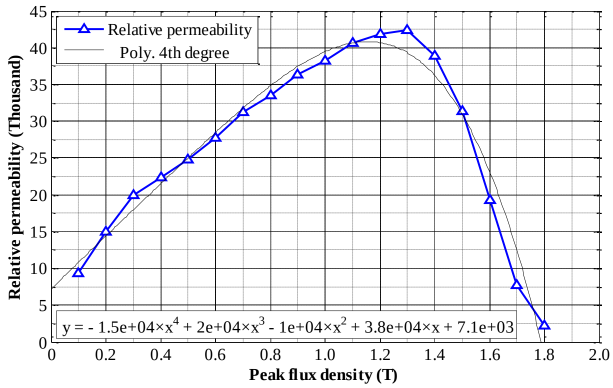

Fig 3 Variation of the effective relative permeability (magnetisation characteristic) of CGO with peak flux density at magnetising frequency 50 Hz

Fig 3 shows that the relative permeability of magnetic laminations varies significantly with peak flux density; therefore magnetisation characteristic of the material is necessary to complete the solution of (2) and extend to a wide range of flux density. Fig 3 also shows that at low flux densities and near saturation, permeability of the material is relatively low and according to (3), at each particular frequency, the impact of skin effect is less compared to the high permeability regions of the curve. In the analytical modelling and experimental parts of this paper, flux density of 1.3 T with μ_r=4.24E+04 was considered as a high permeability point and flux density of 1.7 T with μ_r=7.75E+03 was considered as a low permeability point.

B. Determination of complex relative permeability at high frequencies

Despite the fact that transformer cores and in general magnetic cores work at power frequencies, 50 Hz or 60 Hz, there are situations where the magnetic cores are subjected by high frequency magnetic fields, e.g. transient over-voltages containing high-frequency components and PWM excitations [21]. To analyse these phenomena in magnetic cores, it is convenient to consider the relative magnetic permeability of the material as the complex quantity $\mu_r = \mu_r' - j\mu_r''$ in which μ_r' and μ_r'' are real functions of magnetising frequency f [21]. Therefore in order to improve the accuracy of the analytical modelling at high frequencies, variations in the complex relative permeability over frequency should be observed.

The cross section of the sample of Fig 2 is shown in Fig 4. The size of the lamination sample, given as Δy by Δz, is chosen to be small enough to consider the magnetic field inside it as uniform at low frequencies.

Equation (1) can be written in terms of the magnetic field in the z-direction (rolling direction) H_z as [21]:

$$\frac{\partial^2 \dot{H}_z(x,t)}{\partial x^2} = \mu_0 \mu_z \sigma \frac{\partial \dot{H}_z(x,t)}{\partial t} \tag{9}$$

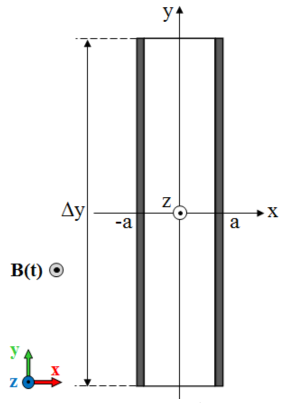

Fig 4 Single strip magnetic lamination of thickness $t=2a$ in x-y plane

Considering the boundary conditions $H_z(\pm a,t) = H_0 e^{j\omega t}$ imposed on each side of the lamination, the magnetic field at any depth inside the lamination can be obtained from (9) as:

$$H_z(x,t) = \frac{H_0}{1+e^{-2\gamma a}}\left(e^{j\omega t-\gamma(x+a)} + e^{j\omega t+\gamma(x-a)}\right) \tag{10}$$

where γ is propagation constant given by $\gamma = \sqrt{j\omega\mu_0\mu_z\sigma}$ which corresponds to the propagation of damped waves from the boundary sides of the lamination $x=\pm a$ in the x direction [21]. The propagation constant is directly related to the skin depth $\delta = 1/\sqrt{\pi\mu_0\mu_z f\sigma}$ by:

$$\gamma = \frac{(1+j)}{2\delta} \tag{11}$$

The averaged magnetic flux density in the z-direction (B_z) can be evaluated in terms of total magnetic flux $\varphi(t)$ through the cross section ($2a\Delta y$) as:

$$B_z(x,t) = \frac{\varphi(t)}{2a\Delta y} = \frac{\int_{-a}^{+a} \mu_0\mu_z H_z(x,t)\Delta y dx}{2a\Delta y} \tag{12}$$

Substituting (10) in (12) and the integrating will lead to:

$$B_z(x,t) = \frac{\mu_0\mu_z H_0 e^{j\omega t}}{a\gamma}\tanh(a\gamma) \tag{13}$$

The effective relative complex permeability of the lamination in z-direction is the ratio of the average flux density to the surface magnetic field intensity. This relationship is given by:

$$\mu_z^{eff} = \mu_z' - j\mu_z'' = \frac{B_z(x,t)}{\mu_0 H_z^{exp}} = \frac{\mu_0\mu_z H_0 e^{j\omega t}}{a\gamma\mu_0 H_0 e^{j\omega t}}\tanh(a\gamma)$$

$$\mu_z^{eff} = \mu_z \frac{\tanh(a\gamma)}{a\gamma} \tag{14}$$

where μ_z' and μ_z'' are real and imaginary parts of the complex relative permeability in the z-direction and are real functions of the frequency. μ_z is the absolute static permeability of the material in the rolling direction which is equal to the value of μ_r at low frequencies [23]. The amplitude and phase angle of the effective complex permeability as a function of the magnetising frequency of CGO *Fe* 3 % *Si* of 0.3 mm thick at two particular surface flux densities 1.3 T and 1.7 T are shown in Fig 5. Conductivity of the material was measured σ=2.17E+06 *S/m* based on the method in [24].

Complex permeability takes into account the influence of skin effect on magnetic properties of the material. At low frequencies, e.g. power frequencies 50 Hz or 60 Hz, this effect is negligible due to the skin depth being significantly greater than the lamination thickness $\delta >> a$. However at high frequencies skin depth becomes noticeable and leads to significant drop in the magnetic permeability of the material. Considering the relation between magnetic flux density $\boldsymbol{B}$ and magnetic field strength $\boldsymbol{H}$, the phase angle of the relative complex permeability represents the phase shift between ***B*** and ***H***. Therefore from Fig 5 it could be concluded that at low frequencies relative complex permeability of the material remains constant and is equal to relative static permeability (μ_r) and also phase shift between ***B*** and ***H*** is almost zero. On the other hand, at high frequencies the amplitude of the relative complex permeability drops significantly and the phase angle becomes noticeable. However since skin effect itself depends on both magnetising frequency and magnetic permeability, variation of the peak flux density influences the profile of the complex relative permeability versus frequency, as the permeability of the material varies with peak flux density. Therefore according to Fig 3, two different behaviours are observed; at high permeability, e.g. 1.3 T, and low permeability at low flux densities and near saturation, e.g. 1.7 T.

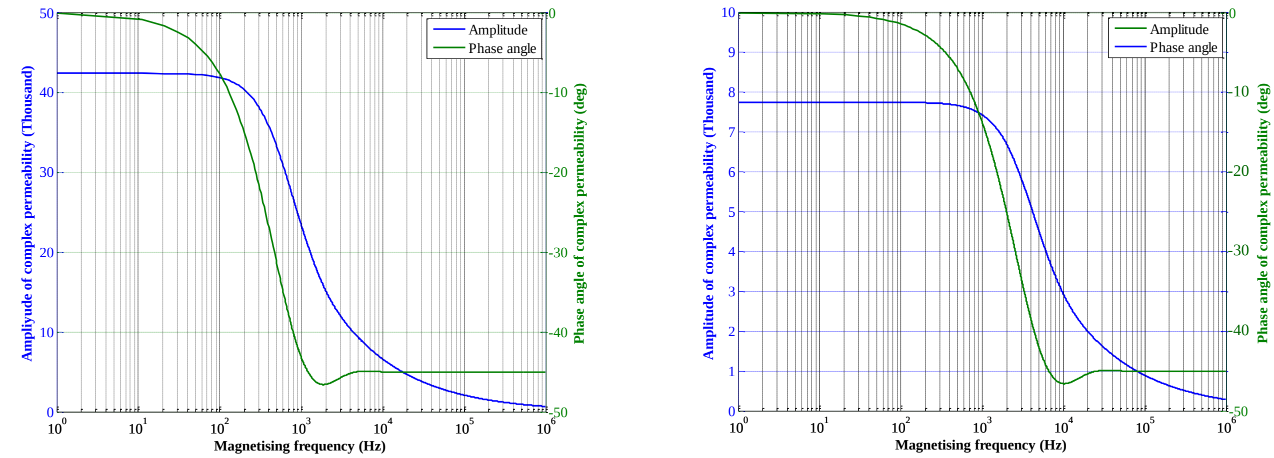

(a) (b)

Fig 5 Complex relative permeability of a single strip magnetic lamination at surface peak flux density (a) B_{pk}=1.3 T and (b) B_{pk}=1.7 T

C. Flux density distribution inside single strip lamination

Based on equation (2) and taking into account the magnetisation characteristic of the material (Fig 3) the distribution of magnetic flux density, normalised by the value at the surface (B_x/B_s), at different depths inside the lamination versus magnetising frequency *f* and two particular surface flux densities 1.3 T and 1.7 T are shown in Figs 6-a and 6-b, respectively. In order to show the impact of the complex permeability on magnetic properties of the material these characteristics were obtained for two magnetic permeabilities: constant and frequency dependent (complex) permeability. The results are shown in Figs 6-a and 6-b.

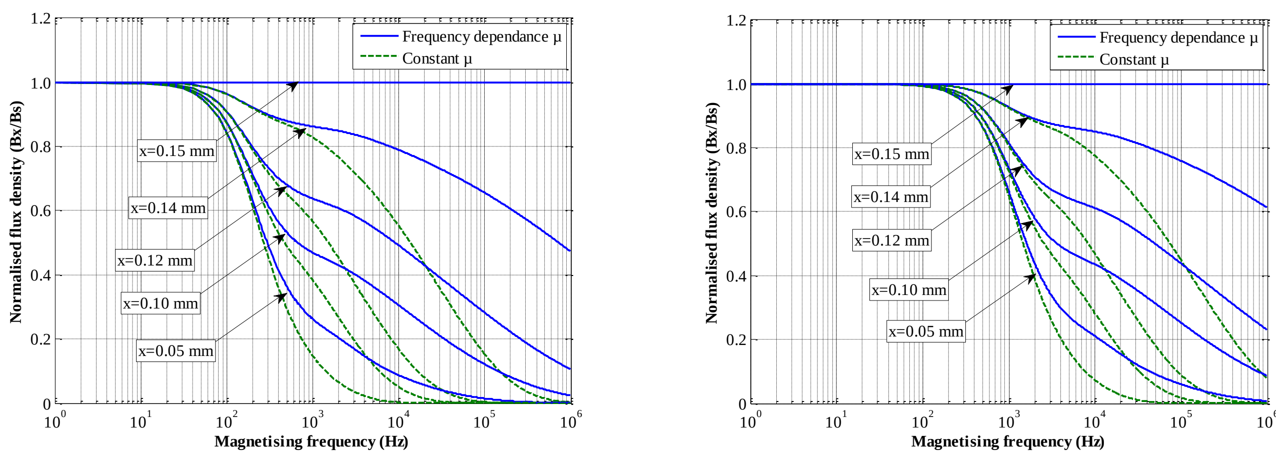

(a) (b)

Fig 6 Normalized magnetic flux density versus magnetising frequency with frequency dependence and constant permeability and different position from lamination surface and peak surface flux densities (a) B_{pk}=1.3 T (b) B_{pk}=1.7 T

Three important points could be concluded from the results of Figs 6-a and 6-b:

1. At low frequencies, where skin effect is negligible, flux density at any depth inside the lamination is constant. At higher frequencies skin effect becomes significant and magnetic flux density decreases with increasing frequency from the surface to the centre of the lamination.
2. From equation (3), at each particular frequency the impact of skin effect is more significant at high values of magnetic permeability; while at low values of magnetic permeability, at low flux densities and near saturation, the impact of skin effect is less and therefore at each particular frequency, flux density at any depth inside the lamination is higher at higher values of magnetic permeability.

3. From equation (14) and Fig 5, complex permeability is a function of skin effect; therefore at low frequencies, the difference between the flux density by constant and complex permeability at each depth inside the lamination is negligible. On the other hand by increasing frequency the impact of skin effect becomes significant and leads to significant different between these two values.

As a final note from Figs 5 and 6, magnetisation characteristic of the material and complex relative permeability are two determinant factors in the study of magnetic properties of the magnetic laminations which will be considered in relevant studies to increase accuracy of the results.

The distribution of normalised magnetic flux density (B_x/B_s) along the lamination thickness for different values of the magnetising frequency f and two particular surface flux densities 1.3 T and 1.7 T were calculated based on equation (2); the results are shown in Figs 7-a and 7-b, respectively.

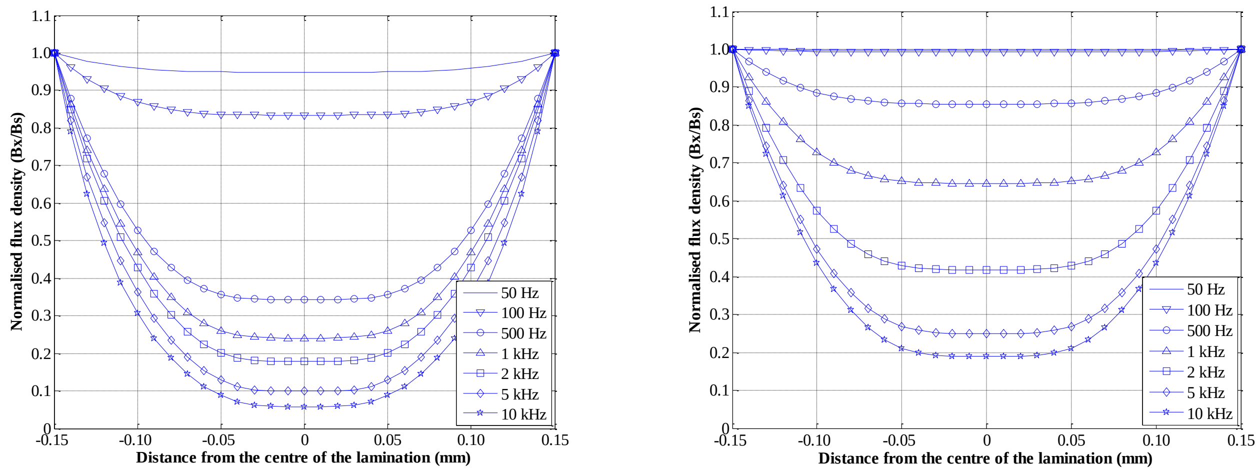

(a) (b)

Fig 7 Normalized magnetic flux density penetration into magnetic lamination of 3 % CGO silicon steel with thickness of $2a$=0.3*mm* at different frequencies (a) B_{pk}=1.3 T (b) B_{pk}=1.7 T

The same conclusions as Fig 6 could be applied to Fig 7. From equation (2), half of the laminations thickness "*a*" and skin depth "*δ*" are the determinant factors in the qualification of the flux density distribution along the lamination thickness. At low frequencies, $\delta >> a$, flux density distributes uniformly along the lamination thickness. However, at high frequencies where $\delta << a$, the flux density at the centre region of the lamination is nearly zero, and corresponding high flux density is noted near the surfaces of the lamination; and hence magnetic flux density distribution tends to be non-uniform across the lamination.

Variation of magnetic permeability is also a determinant factor which affects the distribution of flux density across the lamination. Comparing the corresponding curves of flux density distribution of Figs 7-a and 7-b shows that flux density distribution at low permeabilities is more uniform compared with higher permeabilities; the reason is strongly related to skin effect which is more significant at higher permeabilities. In order to clarify this issue, a 3-D plot of normalised flux density penetration into the lamination, typically at frequency of 500 Hz, and peak flux density from 0.1 T to 1.8 T is shown in Fig 8.

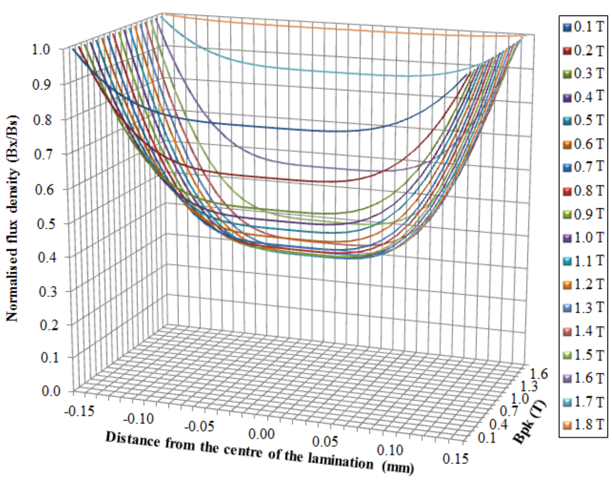

Fig 8 3-D plot of normalized magnetic flux density penetration into magnetic lamination with thickness of $2a$=0.3 *mm* at magnetising frequency of 500 Hz and peak flux density from 0.1 T to 1.8 T

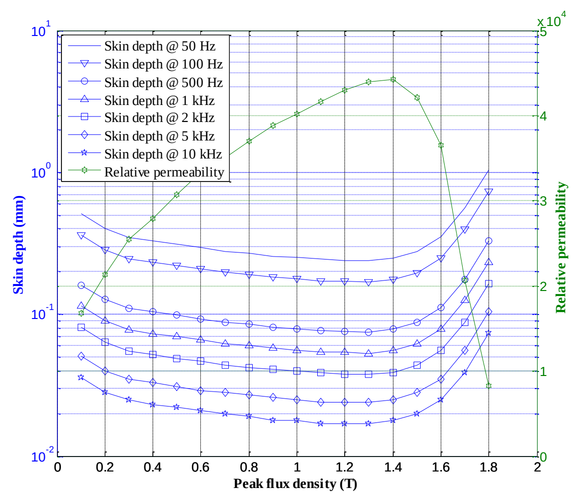

Fig 9 Effect of flux density on relative permeability and skin depth of the magnetic material at magnetising frequencies from 50 Hz up to 10 kHz

Variations of skin depth at different magnetising frequencies from 50 Hz up to 10 kHz together with permeability of the material versus peak flux density are shown in Fig 9. This figure shows significant skin effect at high values of permeabilities; however this effect becomes negligible at low permeabilities at low flux densities and near saturation.

3. EDDY CURRENT POWER LOSS ANALYSIS BASED ON THE EQUIVALENT ELECTRIC CIRCUIT OF THE LAMINATION

The resistance of an object depends primarily on two factors; resistivity of the material and its physical shape. For a given material, with specific electrical resistivity ρ, length l and cross section area of A, the resistance is defined by $R = \rho\, l/A$. The eddy current path in the magnetic laminations which is magnetised by flux density $\boldsymbol{B}$, can therefore be simulated by means of equivalent resistors arranged along the x and the y axis. Fig 10-a shows a perspective view of a magnetic lamination at a flux density $\boldsymbol{B}$ and Fig 10-b shows the equivalent electric circuit of eddy current path.

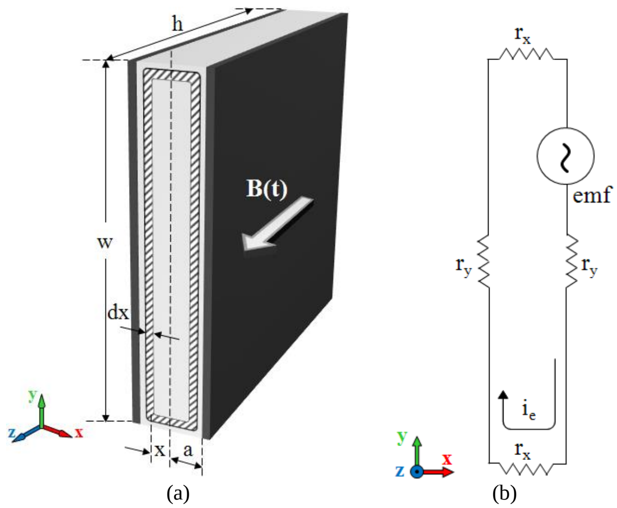

Fig 10 (a) Single strip magnetic lamination (b) equivalent electric circuit of eddy current path [3]

In this figure, R_y and R_x are the Ohmic resistance of the material along the width and thickness of the lamination respectively and *emf* is the induced voltage in the magnetised lamination [3]. As outlined in section 2, at high frequencies where $\delta << a$, impact of skin effect becomes significant which leads to non-uniform distribution of magnetic flux density along the lamination thickness. It therefore affects the eddy current distribution and hence eddy current power loss modelling at high frequencies. Considering this important issue, based on the equivalent circuit of Fig 10-b an analytical model was already developed by the authors [3] to predict eddy current loss of single strip laminations, in a wide range of magnetising frequency and flux density as:

$$p_e = \frac{\pi^2 f^2 B_s^2 wh\delta^3}{2\rho\left(Cosh\,\frac{2a}{\delta} + Cos\,\frac{2a}{\delta}\right)}\left[\frac{4a}{\delta}\left(Cos\,\frac{2a}{\delta} - Cosh\,\frac{2a}{\delta}\right) + Sinh\frac{2a}{\delta}\left(\left(\frac{2a}{\delta}\right)^2 + 2\right) + Sin\frac{2a}{\delta}\left(\left(\frac{2a}{\delta}\right)^2 - 2\right)\right] \qquad (15)$$

In the developed model and proposed procedure, skin effect δ, non-uniform flux density distribution, complex relative permeability and magnetisation characteristic of the material were taken into account. Equation (15) describes the total eddy current power loss of single strip laminations of length h, width w and thickness $2a$ (in Watts) at high frequencies based on the resistive equivalent circuit of the lamination. At low frequencies where $\delta >> a$ and skin effect is negligible, equation (15) tends to:

$$p_e = \frac{4\pi^2 f^2 B_m^2 wha^3}{3\rho} \qquad [W] \qquad (16)$$

which has been known as the conventional equation of eddy current power loss of thin sheet laminations at low frequencies.

A flowchart was designed to calculate the eddy current power loss of magnetic lamination in a wide range of magnetising frequency f and peak flux density B_{pk}, as shown in Fig 11. According to the designed flowchart, the magnetising frequency f and amplitude of the flux density B_{pk} are initially set at the required values.

Relative permeability at the specific peak flux density is then read from the measured values of Fig 3, which is necessary to take the non-linearity of the material into account. Complex relative permeability of the material will be then calculated using equation (14). Local flux density B_x at the specific values of magnetising frequency and amplitude of surface flux density will be then calculated using equation (2); and finally eddy current power loss of the sample will be calculated at the specific frequency and peak flux density using equation (15).

4. RESULTS OF ANALYTICAL MODELLING

In order to investigate the analytical modelling and compare the results, based on the designed flowchart of Fig 11 characteristics of the eddy current power loss versus magnetising frequency obtained by the developed equation of (15) and the conventional equation of (16) at two peak flux densities 1.3 T and 1.7 T are shown in Fig 12. This characteristic was also calculated by equation (15) with constant and frequency dependent values of relative permeabilities; the results are shown in Fig 13. These calculations were performed for a single strip Epstein size magnetic lamination of CGO *Fe* 3 % *Si* of 0.3 mm thick, 30 mm width and 305 mm length with the same magnetic and electric properties as stated in section 2.

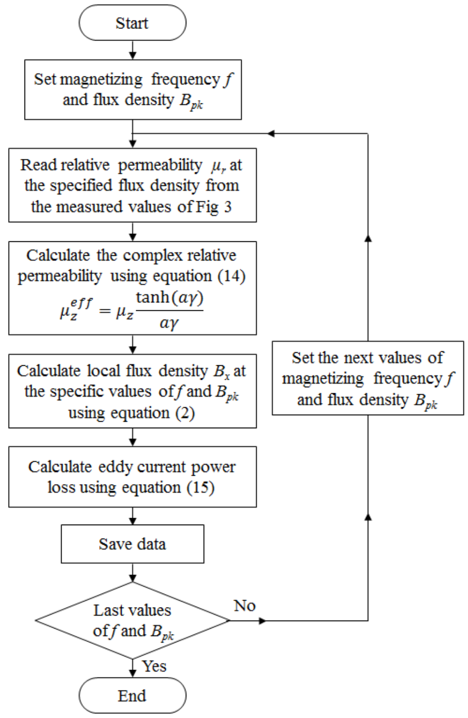

Fig 11 Flowchart of calculation of the flux density distribution

Using equation (16) the whole thickness of the lamination is involved in the resistance of the eddy current path and hence eddy current loss, because this equation was obtained based on uniform flux density distribution through the lamination thickness. However significant skin effect at high frequencies forces eddy currents to flow in a smaller area and increases the resistance of eddy current path. As a consequence, induced eddy current in the lamination and hence eddy current power loss will reduce.

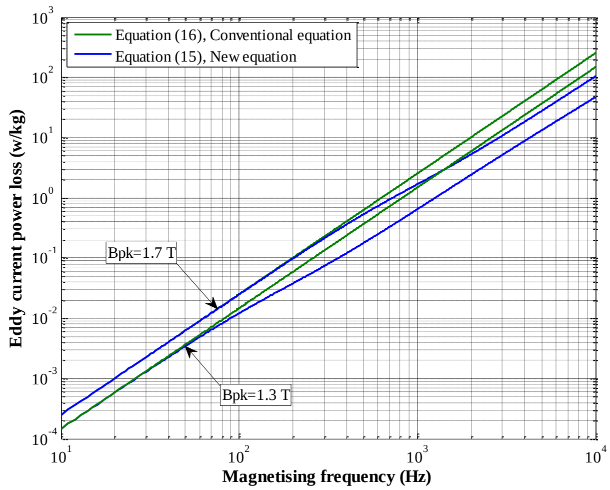

Fig 12 Comparison of eddy current power loss vs. magnetising frequency from conventional equation and new equation at peak flux densities B_{pk}=1.3 T and B_{pk}=1.7 T

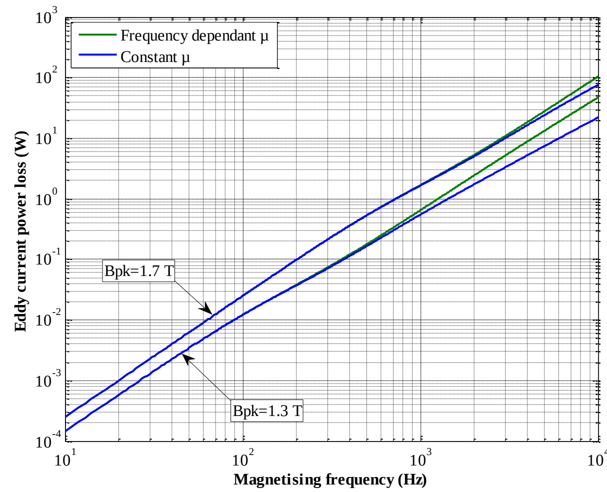

Fig 13 Comparison of eddy current power loss vs. magnetising frequency with constant and frequency dependence relative permeability at peak flux densities B_{pk}=1.3 T and B_{pk}=1.7 T

Fig 12 shows that the difference between eddy current power losses obtained by (15) and (16) increases by increasing the magnetising frequency. This is related to the impact of skin effect on the eddy currents and eddy current power loss. At low frequencies the difference between these two values could be negligible, e.g. the difference at 50 Hz is less than 0.2 %; while this value at 10 kHz is about 60 %. Therefore, Fig 12 shows that at high frequencies the calculated eddy current loss without accounting for skin effect will be an overestimate.

In subsection 2.2 the importance of skin effect on relative permeability of the material at high frequency was shown by means of complex relative permeability. Ignoring this effect leads to higher relative permeability for the material at high frequencies which results in lower eddy current power loss. Fig 13 shows that the difference between the eddy current power losses obtained by constant and frequency dependent relative permeability increases by increasing magnetising frequency; so that for the material with the delineated specifications, the maximum difference between the results at magnetising frequency of 10 kHz is 26.67 %.

Another note that could be concluded from Figs 12 and 13 is related to effect of flux density amplitude on the characteristic. As stated in section 2, at each particular frequency, skin effect is more significant at high values of magnetic permeability. Therefore Figs 12 and 13 show less discrepancy at flux density of 1.7 T with lower permeability and a high discrepancy at flux density of 1.3 T with higher permeability.

5. Core Loss Separation

Magnetic losses of the magnetic cores due to alternating fields have been separated into three categories: hysteresis losses p_h, eddy current losses p_e and anomalous losses or excess loss p_{ex} [25-27]. Thus, total power loss is given by:

$$p_c = p_h + p_e + p_a = k_h f B_{pk}^n + k_e (f B_{pk})^2 + k_{ex} (f B_{pk})^{1.5} \qquad (17)$$

where f is magnetising frequency, B_{pk} is peak flux density, n is constant, k_h , k_e and k_{ex} are hysteresis, eddy current and excess loss coefficients, respectively. Calculating the coefficients of (17) to separate the components of the iron loss is valid within a certain frequency and flux density range [2]. In more recently developed models this range is extended by allowing the coefficients to vary with the frequency and the peak flux density [2], [27-28]. An analytical method, which is known as *extrapolation method*, is usually used to separate the components of core loss using total core loss measurements at different frequencies [28]. In this method the hysteresis loss per cycle is assumed independent of the frequency and the eddy current loss per cycle is assumed as a linear function of frequency. As a practical example, eddy current and hysteresis losses per cycle of an Epstein size single strip lamination (305 mm×30 mm) of CGO was obtained by the extrapolation method at peak flux density 1.5 T and magnetising frequency from 10 Hz to 1000 Hz. The results are shown in Fig 14.

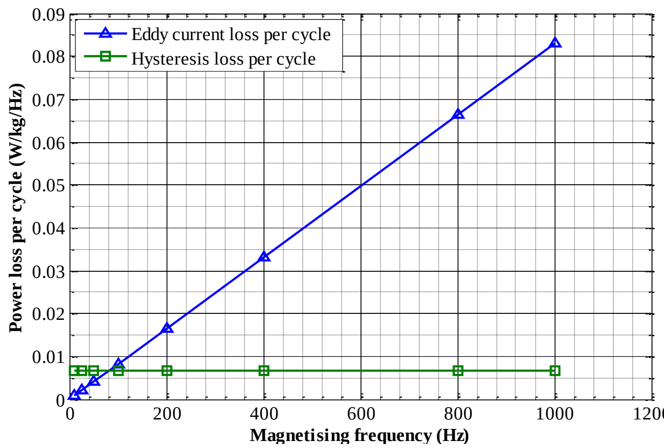

Fig 14 Eddy current and hysteresis power loss per cycle versus frequency obtained by extrapolation method at B_{pk}=1.5 T

As stated in section 2, at high frequencies, skin effect is significant and the peak flux density differs across the lamination thickness. As a result, the local hysteresis loop and the hysteresis loss per cycle vary at each depth inside the lamination. This variation affects the total hysteresis power loss per cycle, making it dependent on the magnetic field distribution, which is strongly affected by the magnetising frequency [2]. Therefore, the separation of core loss components by the extrapolation method, assuming constant hysteresis power loss per cycle, is only valid at low frequencies, where the magnetic field distribution along the lamination is uniform. Accurate core loss separation at high frequencies requires taking non-uniform flux density distribution into account.

Based on the extrapolation method, an experimental-analytical method was developed to separate eddy current power loss from the experimental results accounting for non-uniform flux density distribution and skin effect at high frequencies [3]. In this method in order to improve the coefficients of core loss components the average value of flux density profile along the lamination thickness was considered. Therefore a dimensionless correction coefficient (CC) was defined at each frequency and flux density:

$$CC = \frac{B_{av}}{B_s} \tag{18}$$

where B_s is the flux density at the surface of the lamination and B_{av} is the average value of flux density inside the lamination which is defined by:

$$B_{av} = \frac{1}{2a}\int_{-a}^{a} B(x)\,dx \tag{19}$$

where *2a* is thickness of the lamination and *B(x)* is flux density as a function of distance from the centre line of the lamination which was defined by equation (2). Eddy current loss obtained from the extrapolation method will be then multiplied by the CC defined by equation (18). In order to validate this method, eddy current loss per cycle of the recent practical example was calculated by both the extrapolation and the developed extrapolation methods and the results were compared with that of equation (15). The results are shown in Fig 15.

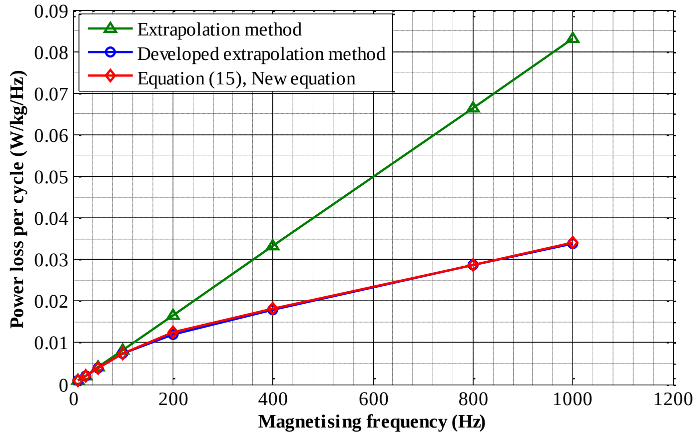

Fig 15 Comparison of eddy current power loss per cycle versus frequency of an Epstein size lamination at B_{pk}=1.5 T obtained from extrapolation method, developed extrapolation method and equation (15)

Fig 15 shows a close agreement between the eddy current power losses per cycle from equation (15) and the extrapolation method at low frequencies, because at low frequencies impact of skin effect is low; however the difference between these two values increases by increasing the magnetising frequency, where at 1000 Hz the difference is about 60 %. On the other hand a close agreement was found between the results of the analytical modelling of equation (15) and the developed extrapolation method at all frequencies, with the maximum difference less about 4 %; because in both methods impact of skin effect and non-uniform flux density distribution have been considered in the relevant procedures. Therefore the developed extrapolation method is a reliable method to separate eddy current power loss component of magnetic cores in a wide range of magnetising frequency.

6. EXPERIMENTAL RESULTS

As a case study, the total power loss of an Epstein size magnetic lamination with 0.3 mm thick CGO *Fe* 3 % *Si* at peak flux densities of 1.3 T, 1.5 T and 1.7 T and magnetising frequency from 10 Hz to 1000 Hz was measured using a single strip tester. A photograph of the measuring system is shown in Fig 16. Principal of the loss measurement is based on the measuring system described in [29]. Results of the measurement are shown in Table I. Based on equations (18) and (19) the correction coefficient of the eddy current power loss of this sample was calculated at each frequency and flux density, the result is shown in Fig 17. The eddy current power loss of the sample was separated at each flux density and frequency based on the developed extrapolation method and the results were compared with the prediction results from the analytical modelling. Magnetisation characteristic of the material and complex relative permeability were considered to predict the power losses. The final results at peak flux densities 1.3 T, 1.5 T and 1.7 T are shown in and Fig 18. The results show a close agreement between the predicted results by the analytical modelling and experimental results of the developed extrapolation method with the maximum difference of less than 4 %.

A. Relation between the CC and skin depth

The results presented in Fig 17 show that the correction coefficient is close to unity at low frequencies and decreases by increasing the magnetising frequency; however, rate of decrease varies with the amplitude of the flux density. According to (18) the correction coefficient of eddy current loss is based on the flux density distribution of Figs 6 and 7 which is related to the impact of skin effect. Furthermore as depicted in Fig 17, at each particular frequency, the correction coefficient at 1.3 T as a high permeability point is lower than its value at 1.7 T as a low permeability point. Therefore based on the results represented in Figs 9 and 17, at each particular frequency a similar variation rate is expected for CC and skin depth versus peak flux density. These characteristics were calculated at two particular frequencies 400 Hz and 1 kHz and flux densities 1.3 T, 1.5 T and 1.7 T for the material with specification of section 2, the results are shown in Fig 19.

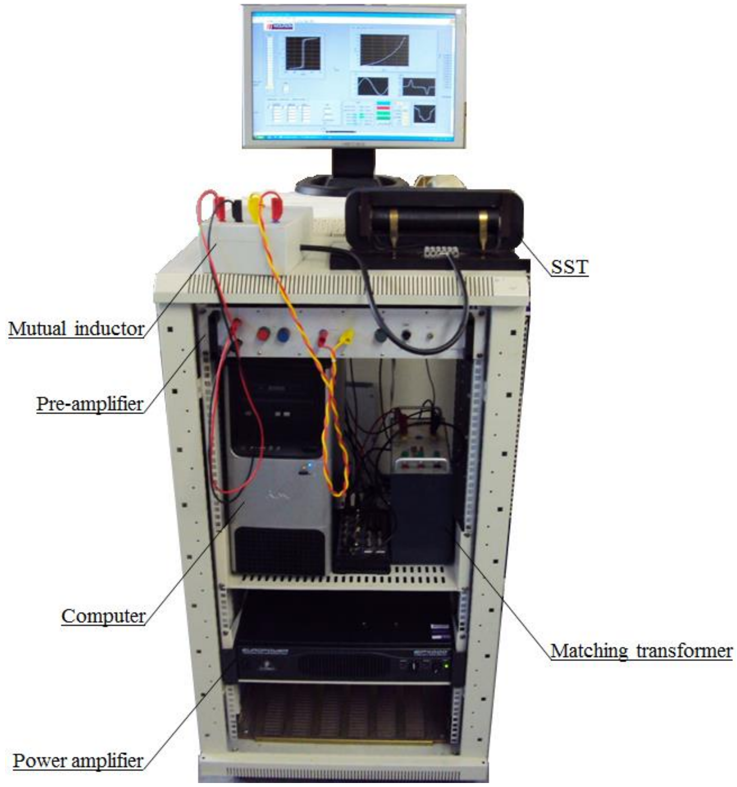

Fig 16 Photographs of measurement system of the single strip tester

Table I Total power loss measurement of an Epstein size lamination of CGO

f (Hz)	**Total power loss, P_t (W/kg)**		
	B_{pk}= 1.3 T	**B_{pk}=1.5 T**	**B_{pk}=1.7 T**
10	0.074	0.107	0.173
25	0.244	0.342	0.520
50	0.674	0.946	1.38
100	1.92	2.61	3.73
200	5.67	7.72	10.9
400	17.5	24.4	34.6
800	57.7	82.8	119
1000	85.6	124	179

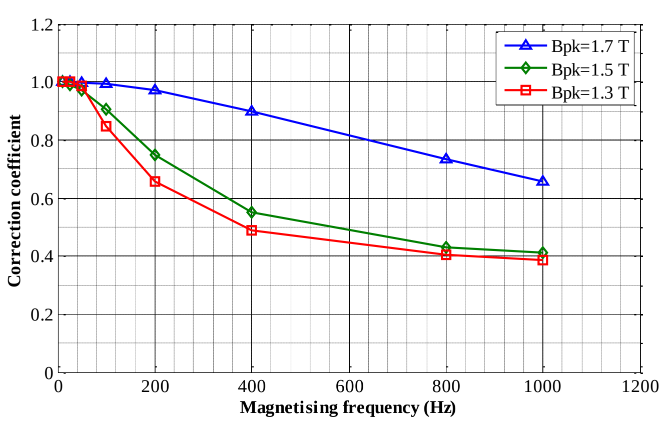

Fig 17 Correction coefficient of eddy current power loss of single strip Epstein size lamination of CGO

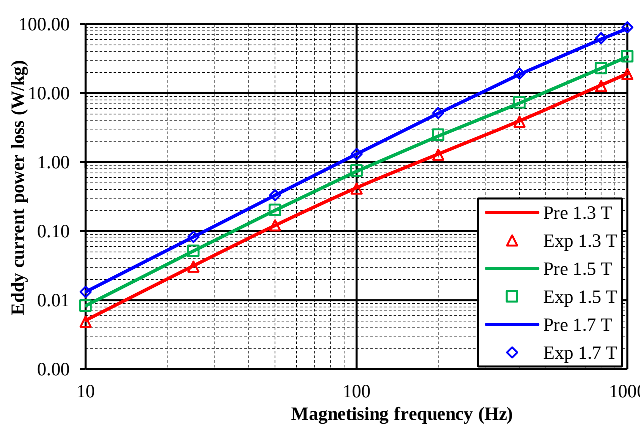

Fig 18 Eddy current power loss of single strip Epstein size lamination of CGO at peak flux densities B_{pk}=1.3 T, B_{pk}=1.5 T and B_{pk}=1.7 T

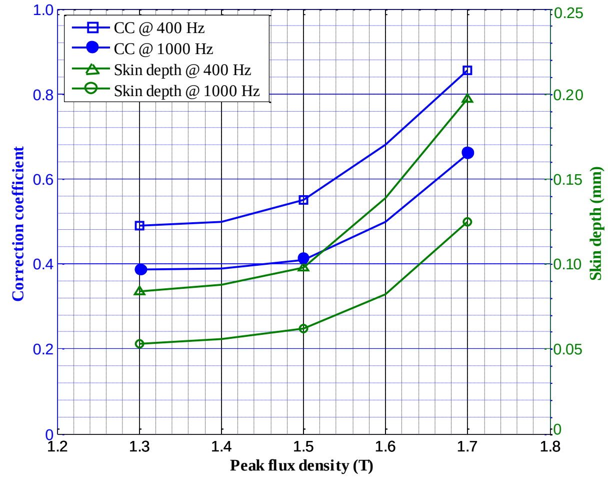

Fig 19 Comparison of correction coefficient of eddy current power loss and skin depth of CGO material versus flux density at 400 Hz and 1 kHz

As expected initially, at each frequency the increasing rate of both skin depth and CC curves are similar, therefore it could be concluded that the correction coefficient of eddy current power loss is a function of skin depth, while skin depth of the material varies with magnetising frequency, relative permeability and amplitude of peak flux density.

7. Conclusion

In this paper an eddy current power loss model was implemented to study the influence of a wide range of magnetising frequencies and relative permeabilities on the magnetic properties of the grain oriented electrical steels. Frequency and relative permeability are two determining factors on skin effect of conductive materials. In magnetic materials skin effect has a significant impact on magnetic properties of materials. For example relative permeability and distribution of flux density along the lamination thickness are strongly affected by skin effect. Based on the analytical modelling it was found that determination of eddy current power loss and separation of loss components in a wide range of magnetising frequency and peak flux density depend on the magnetisation characteristic, non-uniform flux density distribution and complex relative permeability; in which the last two factors are related to skin effect.

In the investigation of the magnetic properties of electrical steels and experimental work on conventional grain oriented (CGO) electrical steel, which is widely used in transformer cores, were used. Samples were magnetised with a time varying magnetic field of magnetising frequency from 10 Hz up to 1000 Hz and peak flux densities of 1.3 T, 1.5 T and 1.7 T. In order to investigate effect of peak flux density on the magnetic properties, peak flux density of 1.3 T was considered as a high permeability point and 1.7 T as a low permeability point. The results highlighted that magnetising frequency and peak flux density are two determinant factors with significant effect on the magnetic properties of electrical steels and should be taken into account in the relevant studies of the magnetic properties of magnetic core. It was also indicated that accurate core loss separation at high frequencies can be achieved by taking into account non-uniform distribution of flux density along the lamination thickness.

Acknowledgment

The authors are grateful to Cogent Power Ltd. for providing the electrical steel sheets and funding this project.

References

[1] G. A. McCo, T. Litman, and J. D. Douglass, "*Energy-Efficient Electric Motor Selection"* Handbook. Portland, OR: Bonneville Power Administration, Jan. 1993, Rev. 3.

[2] M. Ibrahim and P. Pillay, "*Advanced Testing and Modelling of Magnetic Materials Including a New Method of Core Loss Separation For Electrical Machines*", IEEE Transaction on Industry Applications, Vol. 48, NO. 5, Sep/Oct 2012, pp. 1507 – 1515

[3] H. Hamzehbahmani, P. Anderson, J. Hall and D. Fox, "*Eddy Current Loss Estimation of Edge Burr Affected Magnetic Laminations Based on Equivalent Electrical Network-Part II Analytical Modelling and Experimental Results*", IEEE Trans. on Power Delivery, Vol. 29, No. 2, April 2014, pp. 651-659

[4] R. Liu, C. Chunting Mi, and D. Wenzhong Gao, "*Modelling of Eddy-Current Loss of Electrical Machines and Transformers Operated by Pulse-Width-Modulated Inverters*" IEEE Trans. Mag. VOL. 44, NO. 8, August 2008, pp 2021-2028

[5] K. Muramatsu, T. Okitsu, H. Fujitsu, and F. Shimanoe, "*Method of Nonlinear Magnetic Field Analysis Taking Into Account Eddy Current in Laminated Core*" IEEE Trans. Mag. Vol. 40, No. 2, Mar 2004, pp 896-899

[6] Z. Cheng, N. Takahashi, B. Forghani, G. Gilbert, J. Zhang, L. Liu, Y. Fan, X. Zhang, Y.Du, J. Wang and C. Jiao, "*Analysis and Measurements of Iron Loss and Flux Inside Silicon Steel Laminations*", IEEE Trans. Mag. VOL. 45, NO. 3, March 2009, pp 1222-1225

[7] S. E. Zirka, Y. I. Moroz, P. Marketos, A. J. Moses, "*Comparison of Engineering Methods of Loss Prediction in Thin Ferromagnetic Laminations*", Journal of Magnetism and Magnetic Materials 320 (2008) pp 2504–2508

[8] J. Gyselinck, L. Vandevelde, J. Melkebeek, P. Dular, F. Henrotte, and W. Legros, "*Calculation of Eddy Current and Associated Losses in Electrical Steel Laminations*," IEEE Trans. Mag. Vol. 35, No. 3, May 1999, pp 1191-1194
[9] D. A. Jones and W. S. Leung, "*A Theoretical and Analogue Approach to Stray Eddy-Current Loss Laminated Magnetic Cores*," *Proc. Inst. Elect. Eng., Pt. C*, vol. 108, NO. 14, Sep. 1961, pp. 509–515
[10] R. Mazurek, H. Hamzehbahmani, A. J. Moses, P. I. Anderson, F. J. Anayi and T. Belgrand, "*Effect of Artificial Burrs on Local Power Loss In a Three-Phase Transformer Core*" IEEE Trans. Mag. VOL. 48, NO. 4, April 2012, pp 1653-1656
[11] S Mohammadi, M Mirsalim and S Vaez-Zadeh, "*Nonlinear Modelling of Eddy-Current Couplers*" IEEE Trans On Energy Conversion, Vol. 29, No. 1, pp 224-231 March 2014
[12] F. J. Wilkins and A. E. Drake "*Measurements and Interpretation of Power Losses in Electrical Sheet Steel*", Proc. IEE, Vol. 112, No. 4, pp.771 -785 1965
[13] R. Aouli , M. Akroune , M. A. Dami and A. Mouillet "*Iron Loss Measurement Device Under Rotating Magnetic Field*", IEE Proc.-Sci., Meas. Technol., Vol. 146, No. 1, pp.35 -39 1999
[14] A. Canova, and B. Vusini, "*Analytical Modelling of Rotating Eddy Current Couplers*", IEEE Trans. Magn., Vol. 41, No. 1, pp. 24-35, Jan. 2005
[15] A. Geri, A. Salvini and G. M. Veca, "*Displacement Eddy Current Computation in Magnetic Laminates*" IEEE Trans. Mag. VOL. 30, NO. 2, March 1994, pp. 1075-1077
[16] G. Loisos, A. J. Moses, P. Beckley, "*Electrical Stress on Electrical Steel Coatings* "JMMM, 254–255 (2003) pp. 340–342
[17] J. Wang , H. Lin , Y. Huang and L. Huang, "*Numerical Analysis of 3D Eddy Current Fields in Laminated Media Under Various Frequencies*" IEEE Trans. Mag. VOL. 48, NO. 2, February 2012, pp 267-270
[18] S. Mohammadi, M. Mirsalim, S. Vaez-Zadeh, and H. A. Talebi "*Analytical Modelling and Analysis of Axial-Flux Interior Permanent Magnet Couplers*", IEEE Trans. Ind. Electron., Vol. 61, No. 11, pp.5940 -5947, Nov. 2014
[19] S. Mohammadi, and M. Mirsalim, "*Design Optimization of Double-Sided Permanent-Magnet Radial-Flux Eddy-Current Couplers*," Electric Power Systems Research, Vol. 108, pp. 282-292, 2014
[20] F. Brailsford, "*Physical Principles Of Magnetism*", Van Nostrand, 1966
[21] K. Abeywickrama, T. Daszczynski, Y. Serdyuk, and S. Gubanski, "*Determination of Complex Permeability of Silicon Steel For Use In High-Frequency Modelling of Power Transformers*" IEEE Trans. Magn., , Vol. 44, No. 4, Apr. 2008, pp. 438–444
[22] C. A. Schulz, D. Roger, S. Duchesne and J. Vincent, "*E.M.F. Between Magnetic Transformer Sheets: Theoretic Aspects*" in proc. 14th International Symposium on Electromagnetic Fields in Mechatronics, Electrical and Electronic Engineering, Arras, France, September, 2009
[23] V. Leger, C. Ramiarinjaona, R. Barrue and R. Lebourgeois "*Composite Magnetic Materials Based on Nanocrystalline Powders For Middle- And High-Frequency Applications Up To 1 Mhz*" Journal of Magnetism and Magnetic Materials 191 (1999), pp.169-173
[24] P. Anderson, D. R. Jones and J. Hall, "*Measurement of Resistivity of Soft Magnetic Laminations at Elevated Temperatures*", Journal of Magnetism and Magnetic Materials, Vol 304, Issue 2, 2006, pp. e546-e548
[25] Y. Zhang, M.C. Cheng, and P. Pillay, "*A Novel Hysteresis Core Loss Model For Magnetic Laminations*," IEEE Trans. Energy Convers., vol. 26, no. 4, pp. 993–999, Dec. 2011.
[26] G. Bertotti, "*General Properties of Power Losses in Soft Ferromagnetic Materials*," IEEE Trans. Magn. Vol. 24, January1988 pp. 621-630
[27] Y. Chen and P. Pillay, "*An Improved Formula For Lamination Core Loss Calculations in Machines Operating With High Frequency And High Flux Density Excitation*," IEEE 37th IAS Annual Meeting, vol. 2, 13-18 Oct 2002, pp. 759–766
[28] D. M. Ionel, M. Popescu, S. J. Dellinger, T. J. E. Miller, R. J. Heideman, and M. I. McGilp, "*On the Variation with Flux and Frequency of Core Loss Coefficients in Electrical Machine*", IEEE Trans. Magn. Vol. 42, NO. 3, May/June 2006 , pp. 658-666
[29] BS EN 10280:2001 + A1:2007, Magnetic Materials - *Methods of Measurement of The Magnetic Properties of Electrical Sheet And Strip by Means of A Single Sheet Tester*, British Standard, 2007